tvst

DOI: 10.1167/tvst.6.6.4

Article

Polypoidal Choroidal Vasculopathy on Swept-Source Optical Coherence Tomography Angiography with Variable Interscan Time Analysis

Carl B. Rebhun[1,*], Eric M. Moult[2,*], Eduardo A. Novais[1,3], Carlos Moreira-Neto[1,3], Stefan B. Ploner[2,4], Ricardo N. Louzada[1,5], ByungKun Lee[2], Caroline R. Baumal[1], James G. Fujimoto[2], Jay S. Duker[1], Nadia K. Waheed[1], and Daniela Ferrara[1]

[1] New England Eye Center, Tufts University School of Medicine, Boston, MA, USA
[2] Department of Electrical Engineering and Computer Science, Research Laboratory of Electronics, Massachusetts Institute of Technology, Cambridge, MA, USA
[3] Federal University of São Paulo, School of Medicine, São Paulo, Brazil
[4] Pattern Recognition Lab, Friedrich-Alexander-University Erlangen-Nuremberg, Erlangen, Germany
[5] Federal University of Goiás, Goiânia, Brazil

Correspondence: Daniela Ferrara, MD, PhD, Tufts University School of Medicine, 800 Washington Street, Box 450, Boston, MA. e-mail: daniela@ferrara.md

Received: 29 June 2017
Accepted: 6 September 2017
Published: 7 November 2017

Keywords: OCTA; optical coherence tomography angiography; PCV; polypoidal choroidal vasculopathy; variable interscan time analysis

Citation: Rebhun CB, Moult EM, Novais EA, Moreira-Neto C, Ploner SB, Louzada RN, Lee B, Baumal CR, Fujimoto JG, Duker JS, Waheed NK, Ferrara D. Polypoidal choroidal vasculopathy on swept-source optical coherence tomography angiography with variable interscan time analysis. Trans Vis Sci Tech. 2017; 6(6):4, doi:10.1167/tvst.6.6.4

Purpose: To use a novel optical coherence tomography angiography (OCTA) algorithm termed variable interscan time analysis (VISTA) to evaluate relative blood flow speeds in polypoidal choroidal vasculopathy (PCV).

Methods: Prospective cross-sectional study enrolling patients with confirmed diagnosis of PCV. OCTA of the retina and choroid was obtained with a prototype swept-source OCT system. The acquired OCT volumes were centered on the branching vascular network (BVN) and polyps as determined by indocyanine-green angiography (ICGA). The relative blood flow speeds were characterized on VISTA-OCTA.

Results: Seven eyes from seven patients were evaluated. Swept-source OCTA enabled detailed enface visualization of the BVN and polyps in six eyes. VISTA-OCTA revealed variable blood flow speeds in different PCV lesion components of the same eye, with faster flow in the periphery of polyps and slower flow in the center of each polyp, as well as relatively slow flow in BVN when compared with retinal vessels. BVNs demonstrated relatively faster blood flow speeds in the larger trunk vessels and relatively slower speeds in the smaller vessels.

Conclusions: Swept-source OCTA identifies polyps in most, but not all, PCV lesions. This limitation that may be related to relatively slow blood flow within the polyp, which may be below the OCTA's sensitivity. VISTA-OCTA showed heterogeneous blood flow speeds within the polyps, which may indicate turbulent flow in the polyps.

Translational Relevance: These results bring relevant insights into disease mechanisms that can account for the variable course of PCV, and can be relevant for diagnosis and management of patients with PCV.

Introduction

Polypoidal choroidal vasculopathy (PCV), an entity first named by Yannuzzi et al.[1] in 1990, is characterized by a branching vascular network (BVN) terminating in polypoidal lesions and is often accompanied by serous or hemorrhagic retinal pigment epithelium detachment (PED). While fluorescein angiography remains the preferred imaging modality for visualizing typical choroidal neovascularization (CNV), it offers a limited documentation of PCV lesions because these are located below the retinal pigment epithelium (RPE). Indocyanine green angiography (ICGA) is the current gold standard

investigation for the diagnosis of PCV as it allows better visualization of the choroidal vasculature.[2] Both of these standard angiographic techniques are invasive and involve the use of intravenous contrast that can result in systemic adverse events and, rarely, anaphylaxis.[3–5]

Optical coherence tomography (OCT) is a fast and noninvasive imaging modality that plays an important role in the diagnosis and clinical monitoring of PCV lesions.[6,7] Cross-sectional and enface structural OCT suggest the presence of PCV lesions through typical findings such as multiple or multilobulated PEDs, sharp PED peaks, and PED notching,[8] as well as rounded hyporeflective structures correspondent to the polyp lumen. These areas are often seen within the hyperreflective lesions and are adherent to the underside of the RPE. A BVN can also be visualized as a double-layered structure with high reflectivity immediately below the RPE.[9] Despite these characteristic features, it is not always possible to accurately delineate the complete extent of the PCV lesion with structural cross-sectional OCT scans alone, and structural enface OCT is superior in this regard.[10]

OCT angiography (OCTA) is a new OCT-based technology that allows for volumetric and depth-resolved imaging of the retinal and choroidal vasculatures without the need for invasive dyes, by using blood cells as motion contrast.[11,12] OCTA has enjoyed widespread usage in patients with CNV because it allows for visualization of the neovascular complex both above and beneath the RPE without the use of intravenous dye.[11,13–19] There are previous studies showing that the BVN in PCV lesions can be reliably detected using OCTA.[20–24] However, there have been varying reports on the limited sensitivity of OCTA in detecting polyps compared with ICGA.[20–24] It has been hypothesized that slow blood flow in this neovascular complex may be below the sensitivity threshold of OCTA systems to detect blood flow, but this has not yet been confirmed nor demonstrated.[24]

In addition to limited flow sensitivities, current commercial OCTA systems primarily report information pertaining to the presence or absence of blood flow—having velocities within a range defined by the interscan time, which is typically close to 5 ms—but provide little-to-no direct information about flow speeds. This is an unfortunate shortcoming, as knowledge of blood flow speeds may provide further insight into PCV pathophysiology. Recently, an OCTA-based algorithm, termed variable interscan time analysis (VISTA), has been developed by our group for detecting and displaying relative blood flow speeds in the retinal and choroidal vasculatures.[25,26] The aim of the present study is to use high-speed swept-source OCT technology in conjunction with VISTA-OCTA to analyze relative blood flow speeds in PCV lesions.

Methods

This was a cross-sectional, observational study conducted at the New England Eye Center of Tufts Medical Center (Boston, MA) and approved by the Tufts Medical Center and Massachusetts Institute of Technology (Cambridge, MA) institutional review boards. The research adhered to the tenets of the Declaration of Helsinki and complied with the Health Insurance Portability and Accountability Act of 1996. Written informed consent was obtained before swept-source OCT imaging.

Patient Selection

Patients with PCV were seen at the New England Eye Center between August 2015 and January 2016 and prospectively recruited to be imaged on swept-source OCT. Patients were submitted to comprehensive ophthalmologic examination, and the diagnosis of PCV was confirmed by ICGA.

Image Acquisition and Analysis

A high-speed swept-source OCT prototype system, developed at the Massachusetts Institute of Technology, was used in this study. The system uses a vertical cavity surface emitting laser operating at approximately 1050-nm wavelength and 400,000-kHz A-scan rate. For each OCT volume, a total of five repeated B-scans from 500 sequentially, uniformly spaced, slow-scan locations were acquired, with each B-scan consisting of 500 A-scans. The interscan time, accounting for the mirror scanning duty cycle, is approximately 1.5 ms, with the total acquisition time being approximately 3.8 seconds. The axial and transverse resolutions are approximately 8 to 9 μm and approximately 20 μm (full-width-at-half-maximum) in tissue, respectively. For both 3 × 3 mm and 6 × 6 mm, the acquired OCT volumes were centered on the area containing the BVN and polyps, as seen on ICGA. Patients were asked to fixate on an internal target during OCT acquisition. Motion correction was performed using registration of two orthogonally acquired volumes, which are merged into a single volume.[27,28]

A custom C++ application was used for image processing, and ImageJ software (http://imagej.nih.

gov/ij/; provided in the public domain by the National Institutes of Health, Bethesda, MD) was used for visualization. A flat segmentation line was manually adjusted using the orthogonal view, and structural enface and OCTA images were formed by projecting the OCT data through the depths spanned by the lesion.

VISTA-OCTA was performed as previously described.[25,26] In brief, VISTA-OCTA images were formed as follows. First, OCTA images corresponding to 1.5-ms interscan times were formed by comparing temporally adjacent repeated OCT cross-sectional scans; OCTA images correspond to 3-ms interscan times were formed by comparing every other repeated OCT cross-sectional scan. Second, 1.5- and 3-ms interscan time OCTA volumes were projected through the depths spanned by the PCV lesion, thereby yielding 1.5- and 3-ms enface OCTA images. A filtered ratio of these enface images was computed and mapped to a color-coded display. In our VISTA color-coded convention, red indicates relatively fast blood flow speeds and blue indicates relatively slow blood flow speeds.

Two independent readers (EAN and DF) of the Boston Image Reading Center analyzed the 3×3-mm and 6×6-mm enface structural (OCT) and flow (OCTA) images to determine PCV features (e.g., identification of polyps and branching vascular network). VISTA-OCTA images were qualitatively analyzed for blood flow speed information. Disagreement between the two observers was resolved by open adjudication.

Results

Seven eyes from seven patients (5 Asian; 2 African American) were enrolled in this study. The mean age $\pm$ standard deviation of the studied population was 71 $\pm$ 10.2 years. Five patients (71%) were women and two (29%) were men. One patient had a history of enucleation of the contralateral eye because of massive hemorrhage. All subjects had a history of one intravitreal injection of anti–vascular endothelial growth factor in the study eye to manage exudative manifestations of PCV, prior to enrollment in the study.

ICGA identified the presence of BVN, polyps and dilated choroidal vessels in all study eyes. The mean time of identification through vascular filling of BVN and polyp on video ICGA were 25.2 $\pm$ 5.9 and 23 $\pm$ 4.5 seconds.

Swept-source OCTA enabled detailed enface visualization of the BVN in six of seven study eyes (85.7%); visualization of polyps was also possible in six of seven study eyes (85.7%). Corresponding cross-sectional structural OCT scans helped identify the depth and location of the polyps relative to the RPE in all seven study eyes (100%).

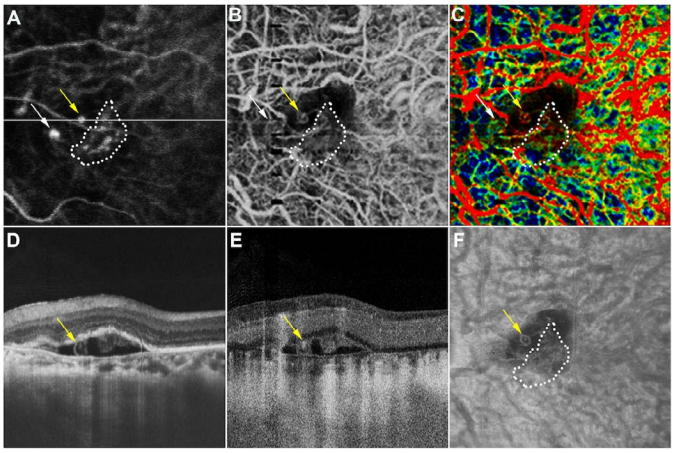

Figure 1. PCV on VISTA-OCTA. Variable blood flow speeds in polyps from the same neovascular complex. Left eye of an 84-year-old woman with PCV. (A) ICGA aligned to the same area as the OCTA and VISTA-OCTA images, demonstrates bright spots corresponding to two polyps (*yellow* and *white arrows*) and a BVN (*white dashed line*). (B) OCTA shows both polyps and the BVN in the same projection. (C) VISTA-OCTA demonstrates variable relative blood flow speeds in two polyps in the same eye. The *yellow arrow* shows a polyp with relatively fast blood flow speed (represented by *red color–coded* OCTA), while the *white arrow* shows a polyp with relatively slow blood flow speed (represented by *green-* and *blue color–coded* OCTA). (D, E) The structural cross-sectional scan and OCTA cross-sectional scan, respectively, taken through the *white line* as seen in (A). The *yellow arrow* points to a polyp. Note that localized decorrelation signal within the polyp in the OCTA cross-sectional scan. (F) Structural enface OCT image shows a polyp and the BVN.

VISTA-OCTA provided information about relative blood flow speeds in all OCTA images in which the BVN and/or polyps were visible. Blood flow speed within polyps varied from polyp-to-polyp within the same eye, as well as from patient-to-patient. Some polyps demonstrated relatively faster flow speeds (red-yellow color-coded velocity range; Fig. 1) while others demonstrated slower flow speeds (blue-green color-coded velocity range; Figs. 2, 3). A common finding was that VISTA-OCTA–derived relative blood flow speeds within a single polyp were not uniform; there was a range of blood flow speeds within a single polyp (Fig. 4). Based on VISTA-OCTA, blood flow in some polyps appeared slower at the center of the polyp, and faster close to the lesion walls (Fig. 1). In all documented eyes, BVNs have

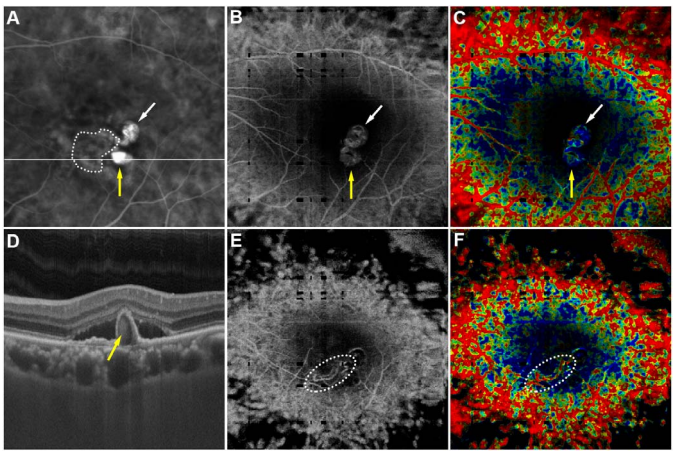

Figure 2. PCV on VISTA-OCTA. Variable blood flow speed within polyp and BVN. Left eye of a 71-year-old man with PCV. (A) Early phase ICGA identifies two polyps and the BVN. Polyps appear as bright spots (*white* and *yellow arrows*). The BVN is demarcated by a *dashed white line*. (B, E) OCTA images of the same eye, but with different projections in order to capture different aspects of the lesion, which occur at different depths of the tissue. (B) Clearly shows both polyps while (E) shows the BVN. (C) VISTA-OCTA image showing relatively slow blood flow speed within the polyps, represented by *blue color–coded* OCTA in both polyps (*white* and *yellow arrows*). (F) A mixture of relatively fast and slow blood flow speeds in the BVN, represented by a range of colors. (D) A structural cross-sectional scan showing a polyp corresponding to the *white line* in (A) and *yellow arrow* in (A–C).

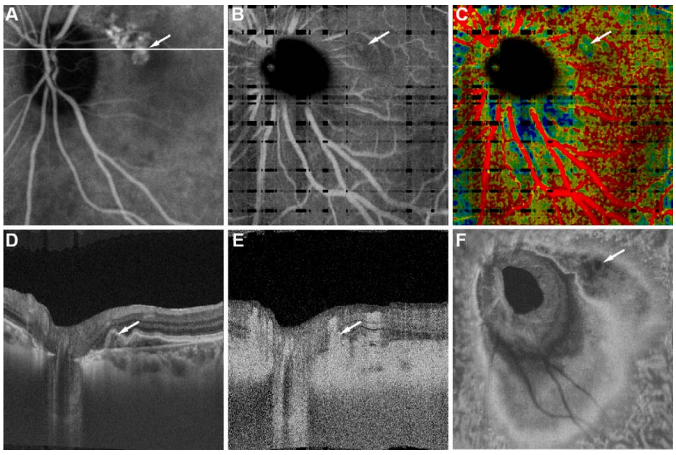

Figure 3. PCV on VISTA-OCTA. Relatively slow flow within the polyp. Left eye of a 62-year-old woman with PCV. (A) ICGA, aligned to the same area as the OCTA and VISTA-OCTA images, demonstrates bright spot corresponding to a polyp (*white arrow*). (B) OCTA shows the polyp (*white arrow*). (C) VISTA-OCTA demonstrates a relatively slow flow (*green-* and *blue–color coded*) within the polyp (*white arrow*). Note the *black gaps* in (B, C) are caused by motion image artifact due to the merging of OCT/OCTA scans in the x and y axis. (D, E) The structural cross-sectional OCT and OCTA scans, respectively, taken through the white line indicated in (A). The *white arrow* points to a polyp. Note the localized decorrelation signal within the polyp in the OCTA cross-sectional scan. (F) Structural enface OCT image shows a polyp as a round hyporeflective area (*white arrow*), surrounded by multilobulated pigment epithelium detachment.

relatively slow flow in comparison to blood flow speed of retinal vessels. Variable blood flow speed was also observed in BVNs, with relatively faster blood flow speeds in the larger trunk vessels and relatively slower speeds in the smaller vessels (Figs. 5, 6).

Discussion

PCV lesions are characterized by polypoidal terminations connected to a BVN.[1,2,29–31] It is still a matter of debate if PCV is a variant of CNV secondary to age-related macular degeneration, or if this is a distinct entity. It has been hypothesized that polypoidal lesions in the vascular terminations occur because of a localized delay in choroidal capillary lobular filling, which causes capillary and venous congestion in the affected lobules. This would impact the RPE–Bruch's membrane complex and produce a PED.[32] The natural history of PCV is widely variable, as well as its response to treatment including anti–vascular endothelial growth factor agents or photodynamic therapy. Large serosanguinous PEDs typically occur in eyes with PCV, and the polyps commonly bleed between the RPE and Bruch's membrane. Intriguingly, self-resolution may also be observed in the natural course of polypoidal lesions.[30,33]

The current gold standard for diagnosing PCV is ICGA, an invasive test with potential risks for the patient.[2,5] OCTA is a noninvasive imaging technology that can separately visualize the retinal and choroidal vasculatures. This technology is increasingly being used to image CNV because it can visualize the neovascular complex both above and beneath the RPE.[11,13–19] However, in recent studies the detection rate of polyps on OCTA compared with ICGA has varied widely, ranging from 45% to 92% detection.[20–22] Interestingly, Tanaka et al.[34] found that OCTA best detected polyps that were observed to be pulsating on video ICGA. In the current study, the polyp detection rate was in the upper range of previously published studies. The longer wavelengths used in the prototype swept-source OCT device might favor the detection of polyps and other choroidal vascular structures, located deeper in the fundus tissue. Such advantage has been previously demonstrated in documenting typical choroidal neovascu-

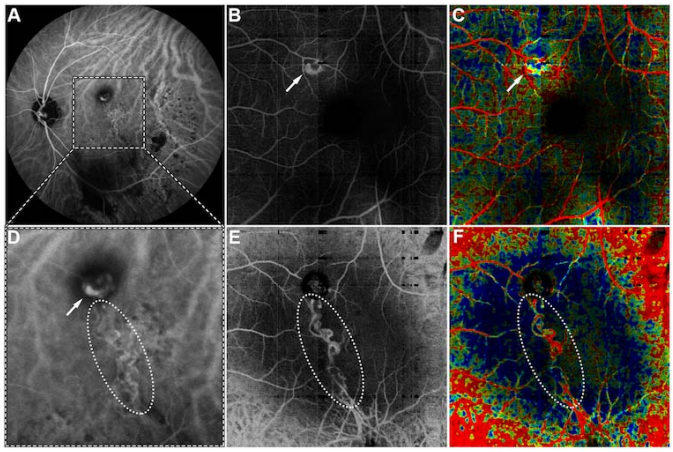

Figure 4. PCV on VISTA-OCTA. Heterogeneous blood flow speed within the polyp. Left eye of a 61-year-old woman with polypoidal choroidal vasculopathy (PCV). (A) ICGA showing the BVN and polypoidal lesion. (D) Larger scale of the macular area documented by ICGA in (A) (*white dashed line*), with the BVN (*white dotted line*) and a polyp with bright periphery toward the polyp wall and dark center (*white arrow*). (B, C, E, F) OCTA images of the same eye, but projected through different axial depths (different segmentation levels) capturing different components of the lesion. (B, C) Clearly shows the polyp with blood flow toward the polyp wall, but not in the center. (E, F) Clearly shows the BVN. The *dark circle* in this segmentation level is caused by blockage artifact in the topography of the polyp, more evident toward the polyp wall (C, F) are OCTA scans applying VISTA-OCTA. (C) Shows relatively slow blood flow speed within the polyp, represented by *green*- and *blue color–coded* OCTA. (F) Shows relatively fast blood flow speed in the BVN, represented by mostly *red color-coded* OCTA.

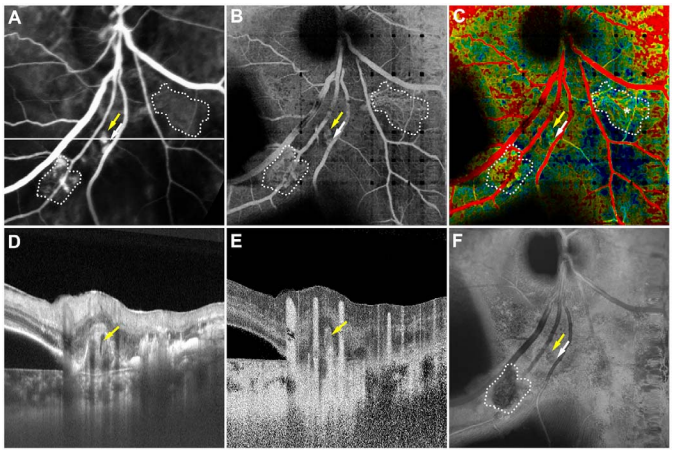

Figure 5. PCV on VISTA-OCTA. Heterogeneous blood flow speed within the BVN. Right eye of a 62-year-old woman with polypoidal choroidal vasculopathy (PCV). (A) ICGA and (B) OCTA identifying two polyps (*yellow* and *white arrows*) and BVN (*white dotted lines*). (C) VISTA-OCTA image shows relatively slow flow within the polyps (*green color–coded* OCTA). A mixture of blood flow speeds within BVN can be seen, but slightly faster flow within a main trunk vessel (*white asterisk*) and relatively slow blood flow speeds at the periphery of the BVN. (D, E) Structural OCT and OCTA cross-sectional scans, respectively, corresponding to the *white line* in (A). (F) The structural enface OCT allows for visualization of the BVN (*white dotted line*) and the polyps (*yellow* and *white arrows*).

larization and choroicapillaris.[19,35–37] While the swept-source OCT technology might contribute to improved rate of polyp detection, the VISTA algorithm on the other hand, does not add to this greater sensitivity. This is because the interscan times used in this study (1.5 and 3 ms) are shorter than those commonly used in standard commercial OCT systems (~5 ms). Thus, all else being equal, the slowest detectable flow using a commercial system should actually be relatively lower than that of our prototype system.

It is important to note that, among the recent literature, the definition of positive identification of polyps on OCTA is a matter of controversy. Some authors consider positive detection of polyps on OCTA as seeing an OCTA decorrelation signal.[38] Other authors have described polyps on OCTA as hyperflow round structure surrounded by hypoflow halo or simply a hypoflow round structure at the level of the choriocapillaris.[21,24] It has been hypothesized that turbulent blood flow within polyps might underlie this variability.[20,21,24,38]

In this study, a prototype high-speed swept-source OCT device was used in conjunction with the VISTA algorithm to visualize variations in relative blood flow speeds within polypoidal lesions. Our data suggests a range of relative blood flow speeds within the polyps and the BVN. This was demonstrated between different components of the lesion in the same eye, and between different eyes. While the mechanism of this variable flow speed is not yet clear, we believe that the relative blood flow speed information provided by VISTA algorithm may inform on the diagnosis of PCV based on OCTA, and may help to elucidate the pathophysiology of PCV. In particular, some polyps appeared to have faster blood flow in the periphery and slower blood flow in the center, which might indicate turbulence within the polyps and might be related to the self-obliteration process occasionally observed in the natural course of the disease. With respect to blood flow speeds within BVNs, our results showed relative faster flow in the larger trunk vessels and slower flow speeds in the smaller vessels. Similar findings have been recently shown in CNV and retinal neovascularization in proliferative diabetic retinopathy using VISTA-OCTA.[26,39] Once treatment para-

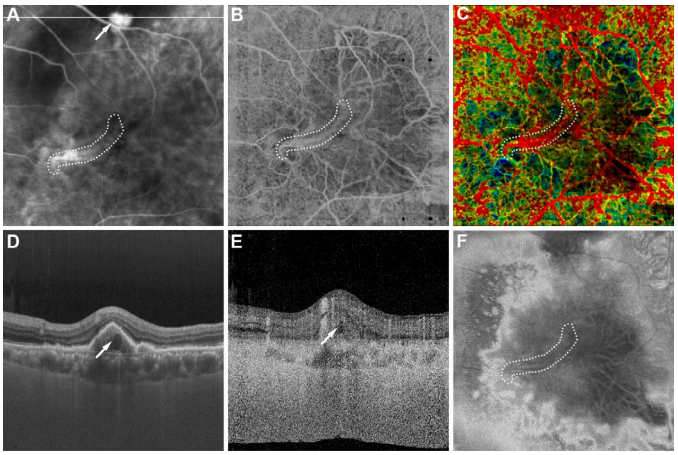

Figure 6. PCV on VISTA-OCTA. Increased blood flow speed within the BVN trunk vessel. Left eye of a 71-year-old man with PCV. (A) ICGA identifies both the BVN trunk vessel (*white dotted line*) and the polyp (*white arrow*), located at different sites. (B) OCTA shows the trunk vessel in the BVN complex (within the *white dotted lines*). No decorrelation signal from the polyp is shown in this OCTA slab. (C) VISTA-OCTA image shows variable blood flow speeds within BVN complex, with faster flow within a main trunk vessel (*white dotted line*) and larger vessels forming a peripheral arcade, and relatively fast-to-moderate blood flow speeds in smaller vessels toward the center of the BVN. (D) Structural cross-sectional OCT corresponding to the *white line* indicated in (A) shows a circular hyporeflective area corresponding to a polyp (*arrow*). (E) Cross-sectional OCTA scan of the same region of (E) shows a low decorrelation signal from the polyp lesion. (F) The structural enface OCT allows visualization of the BVN trunk vessel (*white dotted line*) surrounded by a hyperreflective border that delineates the extension of the neovascular complex within a multilobulated pigment epithelium detachment.

digms are properly established on these new technologies, quantitative assessments of lesion flow may potentially contribute to patient management, informing on lesion activity and potentially indicating response to therapeutic interventions.

Limitations of this study include a relatively small sample size, but the consistency of our observations indicates high reproducibility of the results. The fact that all patients were previously treated with one intravitreal injection of anti–vascular endothelial growth factor raises the question whether naïve-treatment PCV lesions will show similar blood flow patterns, and naïve-treatment lesions should be investigated through the same method in a future study. In addition, we did not establish a direct comparison between ICGA filling speed and VISTA-OCTA–relative flow, as this was not within the scope of this work. There are also limitations with regard to the data processing that preclude a broader use of the strategy employed in this study: the custom software used to process the swept-source OCT data in the present study does not have automated segmentation, and therefore manual adjustment of enface projection boundaries was required to achieve the best quality image, which is time consuming and requires trained assessors. Additionally, in its current form, the VISTA-OCTA algorithm only provides information about relative blood flow speeds (e.g., "the flow in vessel A is faster than that in vessel B"), but not about absolute blood flow speeds (i.e., "the flow in vessel A is 3 mm/s, and that is vessel B is 2 mm/s). Future development of the VISTA algorithm to allow for quantitative measurements of absolute blood flow speed is an important step to enabling further investigation into blood flow speeds in PCV and other clinical presentations of CNV. Finally, there are some factors that might confound the interpretation of VISTA-OCTA. In particular, VISTA-OCTA signals are derived from OCTA signals, which are in turn derived from repeated OCT scans. Thus, artifacts in either the OCT or OCTA imaging can degrade the VISTA-OCTA signal. For example, low OCT signals generates noisy OCTA images, which in turn generate noisy VISTA-OCTA images; similarly, errors in projection ranges, patient motion artifacts, poor optical focusing, and other factors known to corrupt OCTA signal may also corrupt the VISTA-OCTA images.[40] While we have taken measures to reduce the likelihood of such errors, for example, by inspecting coregistered OCT and OCTA data in an orthoplane manner, manually selecting projection ranges, and using a longer wavelength swept-source OCT system that has reduced attenuation artifacts, we have not yet performed formal repeatability analyses of the VISTA-OCTA, particularly in the context of PCV. It is therefore possible that additional imaging artifacts are also present in our dataset.

In conclusion, even though ICGA remains the gold standard for diagnosing PCV, it is invasive and lacks depth resolution.[2,32,41] OCTA is a noninvasive and fast technique for three-dimensional and depth-resolved fundus imaging, allowing different vascular layers of the retina and choroid to be independently documented. Previous studies have had mixed success in identifying polypoidal lesions on OCTA, and, as in our study, found that OCTA was not able to visualize lesions in all cases. VISTA-OCTA, a recently proposed OCTA enhancement that enables visualization of relative blood flow speeds, shows slow and variable blood flow speed in polypoidal lesions, and may increase our understanding of PCV pathophysiology.

Acknowledgments

Supported by grants from the Macular Vision Research Foundation New York, the National Institute of Health (NIH; R01-EY011289-29A, R44-EY022864, R01-CA075289-16), Air Force Office of Scientific Research (AFOSR; FA9550-15-1-0473 and FA9550-12-1-0499), and Thorlabs matching funds to Praevium Research Inc. Additional support came from an unrestricted Research to Prevent Blindness grant and the Massachusetts Lions Clubs, partial supported from Samsung Scholarship from Seoul, South Korea (BKL), and by the Coordination for the Improvement of Higher Education Personnel Foundation within the Ministry of Education of Brazil, Brasilia, Distrito Federal, Brazil (EAN, RNL).

This paper was presented at the Annual Meeting for the Association in Vision and Ophthalmology; May 8, 2017; Baltimore, MD.

*CBR and EMM contributed equally to this manuscript.

Disclosure: **C.B.Rebhun,** None; **E.M. Moult,** intellectual property relating to VISTA; **E.A. Novais,** None; **C. Moreira-Neto,** None; **S.B. Ploner,** intellectual property relating to VISTA; **R.N. Louzada,** None; **B. Lee,** None; **C.R. Baumal,** speaker for Genentech, advisory board for Allergan, consultant for Stealth BioTherapeutics; **J.G. Fujimoto,** stock options in Optovue, royalties from a patent owned by the Massachusetts Institute of Technology and licensed to Optovue, grants from the National Institutes of Health and the Air Force Office of Scientific Research, intellectual property relating to VISTA; **J.S. Duker,** grants from Carl Zeiss Meditec and Optovue, consultant to Allergan, Aura Biosciences, Lumenis Omeros, Santen, Thrombogenics, and Ocudyne, stock holder in Herema Biosciences and Ophthotech, board of directors of Eleven Biotherapeutics and pSivida Corporation; **N.K. Waheed,** grant from the Macula Vision Research Foundation, nonfinancial support from Carl Zeiss Meditec and Topcon, personal fees from Optovue, Nidek, Regeneron, Genentech, Janssen, and Ocudyne; **D. Ferrara,** employed by Genentech, stock/stock options in Roche

References

1. Yannuzzi LA, Sorenson J, Spaide RF, Lipson B. Idiopathic polypoidal choroidal vasculopathy (IPCV). *Retina*. 1990;10:1–8.
2. Spaide RF, Yannuzzi LA, Slakter JS, Sorenson J, Orlach DA. Indocyanine green videoangiography of idiopathic polypoidal choroidal vasculopathy. *Retina*. 1995;15:100–110.
3. Ha SO, Kim DY, Sohn CH, Lim KS. Anaphylaxis caused by intravenous fluorescein: clinical characteristics and review of literature. *Intern Emerg Med*. 2014;9:325–330.
4. Musa F, Muen WJ, Hancock R, Clark D. Adverse effects of fluorescein angiography in hypertensive and elderly patients. *Acta Ophthalmol Scand*. 2006;84:740–742.
5. Garski TR, Staller BJ, Hepner G, Banka VS, Finney RA Jr. Adverse reactions after administration of indocyanine green. *JAMA*. 1978;240:635.
6. Ferrara D, Waheed NK, Duker JS. Investigating the choriocapillaris and choroidal vasculature with new optical coherence tomography technologies. *Prog Retin Eye Res*. 2016;52:130–155.
7. Alasil T, Ferrara D, Adhi M, et al. En face imaging of the choroid in polypoidal choroidal vasculopathy using swept-source optical coherence tomography. *Am J Ophthalmol*. 2015;159:634–643, e632.
8. De Salvo G, Vaz-Pereira S, Keane PA, Tufail A, Liew G. Sensitivity and specificity of spectral-domain optical coherence tomography in detecting idiopathic polypoidal choroidal vasculopathy. *Am J Ophthalmol*. 2014;158:1228–1238, e1221.
9. De Salvo G, Vaz-Pereira S, Keane PA, Tufail A, Liew G. Sensitivity and specificity of spectral-domain optical coherence tomography in detecting idiopathic polypoidal choroidal vasculopathy. *Am J Ophthalmol*. 2014;158:1228–1238, e1221.
10. Sato T, Kishi S, Watanabe G, Matsumoto H, Mukai R. Tomographic features of branching vascular networks in polypoidal choroidal vasculopathy. *Retina*. 2007;27:589–594.
11. de Carlo TE, Bonini Filho MA, Chin AT, et al. Spectral-domain optical coherence tomography angiography of choroidal neovascularization. *Ophthalmology*. 2015;122:1228–1238.
12. de Carlo TE, Romano A, Waheed NK, Duker JS. A review of optical coherence tomography angiography (OCTA). *Int J Retina Vitreous*. 2015;1:5.
13. Jia Y, Bailey ST, Wilson DJ, et al. Quantitative optical coherence tomography angiography of choroidal neovascularization in age-related macular degeneration. *Ophthalmology*. 2014;121:1435–1444.
14. Kuehlewein L, Bansal M, Lenis TL, et al. Optical coherence tomography angiography of type 1

neovascularization in age-related macular degeneration. *Am J Ophthalmol*. 2015;160:739–748, e732.
15. Bonini Filho MA, de Carlo TE, Ferrara D, et al. Association of choroidal neovascularization and central serous chorioretinopathy with optical coherence tomography angiography. *JAMA Ophthalmol*. 2015;133:899–906.
16. Coscas G, Lupidi M, Coscas F, Francais C, Cagini C, Souied EH. Optical coherence tomography angiography during follow-up: qualitative and quantitative analysis of mixed type I and II choroidal neovascularization after vascular endothelial growth factor trap therapy. *Ophthalmic Res*. 2015;54:57–63.
17. Coscas GJ, Lupidi M, Coscas F, Cagini C, Souied EH. Optical coherence tomography angiography versus traditional multimodal imaging in assessing the activity of exudative age-related macular degeneration: a new diagnostic challenge. *Retina*. 2015;35:2219–2228.
18. Moult E, Choi W, Waheed NK, et al. Ultrahigh-speed swept-source OCT angiography in exudative AMD. *Ophthalmic Surg Lasers Imaging Retina*. 2014;45:496–505.
19. Novais EA, Adhi M, Moult EM, et al. Choroidal neovascularization analyzed on ultrahigh-speed swept-source optical coherence tomography angiography compared to spectral-domain optical coherence tomography angiography. *Am J Ophthalmol*. 2016;164:80–88.
20. Inoue M, Balaratnasingam C, Freund KB. Optical coherence tomography angiography of polypoidal choroidal vasculopathy and polypoidal choroidal neovascularization. *Retina*. 2015;35:2265–2274.
21. Wang M, Zhou Y, Gao SS, et al. Evaluating polypoidal choroidal vasculopathy with optical coherence tomography angiography. *Invest Ophthalmol Vis Sci*. 2016;57:OCT526–OCT532.
22. Tomiyasu T, Nozaki M, Yoshida M, Ogura Y. Characteristics of polypoidal choroidal vasculopathy evaluated by optical coherence tomography angiography. *Invest Ophthalmol Vis Sci*. 2016;57:OCT324–OCT330.
23. Kim JY, Kwon OW, Oh HS, Kim SH, You YS. Optical coherence tomography angiography in patients with polypoidal choroidal vasculopathy. *Graefes Arch Clin Exp Ophthalmol*. 2016;254:1505–1510.
24. Srour M, Querques G, Semoun O, et al. Optical coherence tomography angiography characteristics of polypoidal choroidal vasculopathy. *Br J Ophthalmol*. 2016;100:1489–1493.
25. Choi W, Moult EM, Waheed NK, et al. Ultrahigh-speed, swept-source optical coherence tomography angiography in nonexudative age-related macular degeneration with geographic atrophy. *Ophthalmology*. 2015;122:2532–2544.
26. Ploner SB, Moult EM, Choi W, et al. Toward quantitative optical coherence tomography angiography: visualizing blood flow speeds in ocular pathology using variable interscan time analysis. *Retina*. 2016;36(Suppl 1):S118–S126.
27. Kraus MF, Potsaid B, Mayer MA, et al. Motion correction in optical coherence tomography volumes on a per A-scan basis using orthogonal scan patterns. *Biom Opt Express*. 2012;3:1182–1199.
28. Kraus MF, Liu JJ, Schottenhamml J, et al. Quantitative 3D-OCT motion correction with tilt and illumination correction, robust similarity measure and regularization. *Biomedical Opt Express*. 2014;5:2591–2613.
29. Uyama M, Matsubara T, Fukushima I, et al. Idiopathic polypoidal choroidal vasculopathy in Japanese patients. *Arch Ophthalmol*. 1999;117:1035–1042.
30. Uyama M, Wada M, Nagai Y, et al. Polypoidal choroidal vasculopathy: natural history. *Am J Ophthalmol*. 2002;133:639–648.
31. Moorthy RS, Lyon AT, Rabb MF, Spaide RF, Yannuzzi LA, Jampol LM. Idiopathic polypoidal choroidal vasculopathy of the macula. *Ophthalmology*. 1998;105:1380–1385.
32. Costa RA, Navajas EV, Farah ME, Calucci D, Cardillo JA, Scott IU. Polypoidal choroidal vasculopathy: angiographic characterization of the network vascular elements and a new treatment paradigm. *Prog Retin Eye Res*. 2005;24:560–586.
33. Cheung CMG, Yang E, Lee WK, et al. The natural history of polypoidal choroidal vasculopathy: a multi-center series of untreated Asian patients. *Graefes Arch Clin Exp Ophthalmol*. 2015;253:2075–2085.
34. Tanaka K, Mori R, Kawamura A, Nakashizuka H, Wakatsuki Y, Yuzawa M. Comparison of OCT angiography and indocyanine green angiographic findings with subtypes of polypoidal choroidal vasculopathy. *Br J Ophthalmol*. 2017;101:51–55.
35. Told R, Ginner L, Hecht A, et al. Comparative study between a spectral domain and a high-speed single-beam swept source OCTA system for identifying choroidal neovascularization in AMD. *Sci Rep*. 2016;6:38132.

36. Lane M, Moult EM, Novais EA, et al. Visualizing the choriocapillaris under drusen: comparing 1050-nm swept-source versus 840-nm spectral-domain optical coherence tomography angiography visualizing the choriocapillaris under drusen. *Invest Ophthalmol Vis Sci*. 2016;57(9):OCT585–OCT590.
37. Miller AR, Roisman L, Zhang Q, et al. Comparison between spectral-domain and swept-source optical coherence tomography angiographic imaging of choroidal neovascularization imaging of CNV With SS-OCTA and SD-OCTA. *Invest Ophthalmol Vis Sci*. 2017;58:1499–1505.
38. Dansingani KK, Balaratnasingam C, Naysan J, Freund KB. En face imaging of pachychoroid spectrum disorders with swept-source optical coherence tomography. *Retina*. 2016;36:499–516.
39. Rebhun CB, Moult EM, Ploner S, et al. Analyzing relative blood flow speeds in choroidal neovascularization using variable interscan time analysis OCT angiography. *Ophthalmology Retina*. In Press.
40. Ferrara D. Image artifacts in optical coherence tomography angiography. *Clin Exp Ophthalmol*. 2016;44:367–368.
41. Stanga PE, Lim JI, Hamilton P. Indocyanine green angiography in chorioretinal diseases: indications and interpretation: an evidence-based update. *Ophthalmology*. 2003;110:15–21; quiz 22–13.